ATP Release through Connexin Hemichannels in Corneal Endothelial Cells

Priya Gomes,[1] *Sangly P. Srinivas,*[2] *Willy Van Driessche,*[1] *Johan Vereecke,*[1] *and Bernard Himpens*[1]

Purpose. Intercellular Ca^{2+} wave propagation is a distinct form of cell–cell communication. In corneal endothelial cells, intercellular Ca^{2+} wave propagation evoked by a point mechanical stimulus (PMS) is partially mediated by adenosine triphosphate (ATP) release and subsequent activation of P2Y receptors. This study was conducted to investigate the possibility that extrajunctional connexons (hemichannels) play a role in ATP release during PMS-induced Ca^{2+} wave propagation in bovine corneal endothelial cells (BCECs).

Methods. A Ca^{2+} wave was evoked by a PMS applied to a single cell in a monolayer of cultured BCECs. Changes in $[Ca^{2+}]_i$ in the mechanically stimulated cell (MS cell) and in the neighboring (NB) cells were visualized by fluorescence imaging using the Ca^{2+}-sensitive dye Fluo-4. From these images, the maximum normalized fluorescence (NF), the percentage of responsive cells (%RC), and the total area of cells reached by the Ca^{2+} wave (active area [AA], in square micrometers) were calculated. Intercellular dye transfer, generally attributed to gap junctional coupling, was assessed by fluorescence recovery after photobleaching (FRAP) using 6-carboxyfluorescein diacetate. Opening of hemichannels was investigated by measuring cellular uptake of the fluorescent dye Lucifer yellow, which is known to permeate hemichannels. ATP release was measured by luciferin-luciferase bioluminescence.

Results. Flufenamic acid (FFA; 50 μM) and the connexin mimetic peptide Gap26 (300 μM), known blockers of hemichannels, significantly reduced AA in confluent monolayers as well as in contact-free cells. Neither FFA nor Gap26 affected the FRAP, indicating that reduction in AA of the PMS-induced wave by these agents is not due to a block of gap junction channels. FFA as well as Gap26 inhibited the increase in AA of the wave that was observed when cells were pretreated with the ectonucleotidase inhibitor ARL-67156 (100 μM). These findings suggest that the hemichannel blockers reduce the Ca^{2+} wave propagation by inhibiting ATP release. Consistent with this finding, PMS or exposure to Ca^{2+}-free solution (a maneuver known to induce the opening of hemichannels) led to ATP release; moreover, the release was inhibited by the hemichannel blockers. The extracellular ATP levels in response to both PMS and extracellular Ca^{2+} removal were strongly enhanced by ARL-67156, and this effect was inhibited by FFA as well as by Gap26. Moreover, pretreatment of subconfluent BCEC monolayers with FFA or Gap26 inhibited the uptake of Lucifer yellow induced by removal of extracellular Ca^{2+}.

Conclusions. Hemichannels contribute to ATP release on mechanical stimulation in BCECs. The released ATP contributes to propagation of the Ca^{2+} wave. (*Invest Ophthalmol Vis Sci.* 2005;46:1208–1218) DOI:10.1167/iovs.04-1181

The phenomenon of intercellular Ca^{2+} wave propagation represents a distinct form of cell–cell communication and has been demonstrated to involve at least two mechanisms: exchange of inositol 1,4,5-trisphosphate (IP_3) or Ca^{2+} through gap junctions and/or adenosine triphosphate (ATP) release and subsequent activation of the P2Y receptors of the neighboring cells.[1] The importance and existence of these two mechanisms have been investigated in many cell types by inducing Ca^{2+} waves through an acute intracellular photorelease of caged IP_3 or by point mechanical stimulation (PMS) of a single cell with a blunt micropipette.[2,3] A recent study from our laboratory,[4] which focused on Ca^{2+} wave propagation in bovine corneal endothelial cells (BCECs), demonstrated that PMS produces a transient Ca^{2+} increase in the mechanically stimulated (MS) cell followed by a decremental Ca^{2+} wave that propagated across four to six neighboring (NB) cell layers. Similar findings have been reported in several cell types including astrocytes, epithelial cells, fibroblasts, and vascular endothelium.[5–8] The PMS-induced intercellular Ca^{2+} waves in BCECs were partially suppressed by suramin (a nonselective P2Y receptor antagonist) and by exogenous apyrases and were enhanced by exposure to ARL-67156 (an ectonucleotidase inhibitor).[4] Together, these findings provide evidence for an involvement of extracellular ATP in the PMS-induced wave propagation.[4]

In addition to being involved in intercellular communication (also see Ref. 9), activation of purinergic receptors by ATP resulting in elevation of $[Ca^{2+}]_i$ and/or activation of PKC, is known to influence several physiological and pathophysiological processes, including activation of ion channels,[10] contraction of smooth muscles cells,[11] altered barrier integrity,[12] fluid transport,[13] enhanced regulatory volume decrease,[14,15] cell proliferation,[16–19] apoptosis,[20] and inflammation.[21] Given these pleiotropic effects, the release of ATP and its role as a paracrine–autocrine mediator, has been intensively investigated.[22,23] Although release of ATP in response to mechanical stimulation was first documented during sustained exercise of human forearm muscle,[24] the widespread occurrence and significance of such a release was not realized until recently. ATP released from red blood cells in response to mechanical deformation is believed to regulate vascular resistance. ATP is also released from vascular endothelial cells during periods of increased blood flow, shear stress, and hypoxia.[25] After release, ATP, acting as an autocrine–paracrine mediator, can activate endothelial P2Y receptors and stimulate the synthesis of nitric oxide.[26] Also, enhanced ATP release from the urothelium of the rabbit urinary bladder as a consequence of distention by small changes in hydrostatic pressure has been reported.[27] It has been proposed that such a release of ATP from the urothe-

From the [1]Laboratory of Physiology, Catholic University of Leuven, Leuven, Belgium; and the [2]School of Optometry, Indiana University, Bloomington, Indiana.

Supported by National Eye Institute Grants EY11107 and EY14415 (SPS); FWO-Vlaanderen G.0218.03, GOA/2004/07, IAP program 5/05 (BH, JV); and IRO Catholic University of Leuven (PG).

Submitted for publication October 6, 2004; revised December 8, 2004; accepted December 16, 2004.

Disclosure: **P. Gomes**, None; **S.P. Srinivas**, None; **W. Van Driessche**, None; **J. Vereecke**, None; **B. Himpens**, None

The publication costs of this article were defrayed in part by page charge payment. This article must therefore be marked "*advertisement*" in accordance with 18 U.S.C. §1734 solely to indicate this fact.

Corresponding author: Johan Vereecke, Laboratory of Physiology, K. U. Leuven, Campus Gasthuisberg O/N, B-3000 Leuven, Belgium; johan.vereecke@med.kuleuven.ac.be.

lium acts as a sensory mediator of the degree of distension of the urinary bladder.[27] Autocrine–paracrine signaling through the release of ATP has also been found to occur in rat hepatocytes.[28] ATP release in response to mechanical stimulation and activation of P2Y receptors also appears to be important for cell volume regulation in swollen hepatocytes and related cell lines. Similarly, hypotonic stimulation of cultured ocular ciliary epithelial cells led to a threefold increase of the extracellular ATP concentration.[29] This may be important in the regulation of intraocular pressure, because ATP and its metabolite adenosine have been implicated in the regulation of ciliary epithelial Cl^- conductance and formation of aqueous humor.[30]

Although release of ATP is well documented, pathway(s) for the release are yet to be ascertained. Given the diversity of conditions and cell types in which ATP is known to be released (see review by Lazarowski et al.[31]), several pathways could be involved in the release of ATP and other nucleotides. Several studies have suggested that nucleotides are released during cargo–vesicle trafficking and/or by exocytosis.[31] Other suggested pathways include the ATP-binding cassette (ABC) transporters, such as cystic fibrosis transmembrane conductance regulator (CFTR) and the product of the MDR-1 gene[32]; the P-glycoprotein; or stretch and voltage-gated channels, such as plasmalemmal voltage-dependent anion channel (pl-VDAC; a murine splicing variant of the mitochondrial ATP porin VDAC-1)[33] and the stretch-activated cation channels. Recently, Stout et al.[34] provided evidence for the involvement of hemichannels in ATP release during PMS-induced Ca^{2+} wave propagation in astrocytes. Similar findings have been reported by Braet et al.[35] based on Ca^{2+} waves induced by photorelease of IP_3.

Hemichannels represent "pores" formed by a characteristic hexameric assembly of connexin subunits. Fully assembled hemichannels are exocytosed to the plasma membrane in their closed state. Such hemichannels associate (dock) with their counterparts on the apposing cell. Favorable docking of hemichannels from two apposing cells leads to formation of a conductive pore, referred to as the gap junctional channel. This channel connects the cytoplasm of the two neighboring cells through a pathway that has relatively nonselective permeability to a variety of substances of up to ~1500 Da. A significant number of recent studies have endorsed the view that hemichannels may operate as independent channels in the plasma membrane (for example, Ref. 36). Given that the open probability of hemichannels is affected by metabolic ATP depletion,[37] corneal hypoxia can be expected to influence the activity of hemichannels in corneal endothelium, leading to ATP release. This may exacerbate ATP depletion, and also influence the endothelial membrane potential, cell volume and HCO_3^- transport through autocrine–paracrine activity of the released ATP.

The principal objective of this study was to examine the ATP release pathway involved in the spread of the Ca^{2+} wave observed in response to a PMS of a single cell in confluent monolayers of cultured BCECs. The results showed that both the Ca^{2+} wave and ATP release were inhibited by putative hemichannel blockers, consistent with the view that one of the pathways of ATP release involves hemichannels.

Materials and Methods

Cell Culture

Primary cultures of BCECs were established as previously described.[38–40] The growth medium contained Dulbecco's modified Eagle's medium (DMEM, 11960-044; Invitrogen-Gibco, Karlsruhe, Germany) supplemented with 10% fetal bovine serum (F-7524; Sigma-Aldrich, Deisenhofen, Germany), 6.6% L-glutamine (Glutamax; 35050-038; Invitrogen-Gibco), and 1% antibiotic-antimycotic mixture (15240-096; Invitrogen-Gibco). Cells were grown at 37°C in a humidified atmosphere containing 5% CO_2. Cells of the second and third passages were harvested and seeded into two-chambered glass slides (155380, Laboratory-Tek; Nunc, Rosklide, Denmark) at a concentration of 165,000 cells per chamber (4.2 cm^2), unless stated otherwise. Cells were allowed to grow to confluence for 3 or 4 days before use.

Mechanical Stimulation

PMS consisted of a brief deformation of the cell by briefly touching <1% of the cell membrane with a glass micropipette (tip diameter, <1 μm) using a piezoelectric crystal mounted on a micromanipulator (Piezo device P-280, Amplifier-E463; PI Polytech, Karlsruhe, Germany) that undergoes a mechanical deformation when subjected to a voltage, allowing small reproducible displacements of the pipette in response to application of a voltage to the crystal.

Measurement of $[Ca^{2+}]_i$

Cells were loaded with the Ca^{2+}-sensitive fluorescent dye Fluo-4 AM (10 μM) for 30 minutes at 37°C. The fluorescence was measured on a confocal laser scanning microscope (model LSM510; Carl Zeiss Meditec, Jena, Germany). The dye was excited at 488 nm, and fluorescence emission at 530 nm was collected with a 40× objective, unless stated otherwise. Images with a frame size of 106,080 μm^2 were acquired at a resolution of 128 × 128 pixels and 256 gray levels. Polygonal regions of interest (ROIs) were drawn to define the borders of each cell. In the figures and discussions to follow, the NB cells immediately surrounding the MS cell are referred to as NB1 (signifying neighboring cell layer 1). Cells immediately surrounding the NB1 cells are referred to as NB2 cells, and so on. Fluorescence was averaged over the area of each ROI. The maximum normalized fluorescence (NF) was then obtained by dividing the maximum fluorescence on PMS by the basal fluorescence. Intercellar Ca^{2+} wave propagation was characterized in terms of maximum NF, %RC, and the total surface area of responsive cells with NF ≥ 1.1, called the active area (AA).

In some experiments, a cell-free region (referred to as the cell-free lane) was made by scraping off a narrow line of cells in the monolayer using a sharp needle. The cell-free lane was approximately 75 μm wide, corresponding to the width of two to three cells and divided the monolayer into two unconnected regions. Ca^{2+} wave propagation was then studied upon stimulation of a cell at the border of the cell-free region. The side with the MS cell is referred to as the mechanically stimulated side, and the opposite side of the cell-free lane is called the other side. Separate AAs were measured at each side of the cell-free lane.

Fluorescence Recovery after Photobleaching

Cells were loaded with the Ca^{2+}-insensitive dye 6-carboxyfluorescein diacetate (10 μM) for 5 minutes at room temperature, and fluorescence recovery after photobleaching (FRAP) was measured with the laser scanning microscope (LSM510; Carl Zeiss Meditec). The dye was excited at 488 nm, and its emission was recorded at 570 nm. A neutral-density filter was used to minimize photobleaching.

Before bleaching, polygons were drawn around the cells chosen for bleaching, and two prebleach images were scanned. The cells chosen for bleaching were then exposed to 50 scans with the laser at 95% intensity, and the recovery of fluorescence in the bleached cells was measured every 10 seconds over a period of 5 minutes. The decrease of fluorescence in a square region of interest widely distant from the bleached cells was measured as a reference for correction for background bleaching due to the scanning light. After correction for background bleaching, the recovery of fluorescence in the bleached cell at 3 minutes was compared with that of the prebleach scan, and the percentage recovery was calculated. In each experiment, three cells in widely separated areas of the monolayer were chosen for bleaching, and three experiments were performed in each monolayer.

Lucifer Yellow Uptake

Monolayers of cells were incubated for 5 minutes in Ca^{2+}-rich or Ca^{2+}-free solution, each of which contained 5% Lucifer yellow (LY; 432 Da; a hydrophilic anionic fluorescent dye). Uptake of the dye into cells was detected by fluorescence imaging using the confocal microscope (LSM510; Carl Zeiss Meditec). LY was excited at 488 nm, and its emission was recorded at 530 nm. Images with a frame size of 106,080 μm^2 were acquired at a resolution of 512 × 512 pixels and 256 gray levels.

ATP Measurements

ATP measurements were performed with the luciferin–luciferase (LL) bioluminescence assay.

Perfusion Experiments. In the experiments to study the effects of Ca^{2+}-free solution and FFA on ATP release, a setup for measuring luminescence was used as described by Jans et al.[41] The apparatus was equipped with a photon-counting photomultiplier tube (25-mm diameter; H3460-04; Hamamatsu Photonics, Hamamatsu, Japan) held 20 mm above the surface of the cells. The output of the photomultiplier tube in the form of voltage pulses was counted with a high-speed timer-counter interface (PCI-6601; National Instruments Corp., Austin, TX). This setup made it possible to perfuse the cells and to change perfusate without interrupting photon counting.[41] To measure the accumulated ATP released by the cells, a solution containing LL was applied, and the perfusion was stopped temporarily for 1.5 minutes during which period luminescence was measured. Thereafter, perfusion of the cells was resumed with solutions without LL.

Experiments with Complete Intermittent Renewal of Solution. Because continuous perfusion experiments as indicated earlier would be very expensive when Gap26, ARL-67156, or apyrase was required in the perfusate, the effects of these substances were examined without perfusion of the chamber. For this purpose, a separate photon-counting setup was built also using a photomultiplier tube (Hamamatsu Photonics) and a high-speed timer-counter interface (PCI-6601; National Instruments Corp., Austin, TX). LL was added to the bathing solution, and the luminescence counts were measured. Immediately after the luminescence measurements, the solution was gently replaced with a fresh solution without LL. These experiments were performed in the presence of ARL-67156 to inhibit the hydrolysis of ATP by ecto-adenosine triphosphatases (ATPases).

Experiments with Sampling. Experiments with ATP measurement after PMS were performed on the confocal microscope. Samples of 25 μL of the 500-μL bathing solution were taken at different times and quickly transferred to the separate photon-counting setup, where the luminescence was measured after adding LL to each of the samples. Results of consecutive ATP measurements were corrected for the volume of extracellular fluid removed in previous samples.

Calibration of ATP Measurements. Calibration curves of luminescence count versus ATP were obtained at known concentrations of ATP in the presence of 50 μL/mL LL reagent dissolved in the same solutions as used in the experiments. Calibration experiments showed that EGTA (2 mM) increased the luminescence sensitivity by 50%, whereas FFA (50 μM) decreased the sensitivity by 30%. Gap26 (300 μM) and ARL-67156 were without any effect. The data of all experiments with ATP measurements were corrected on the basis of the calibration curves.

Chemicals

Fluo-4 AM and 6-carboxyfluorescein diacetate were obtained from Molecular Probes (Eugene, OR). Flufenamic acid (FFA), ARL-67156 (6-*N*,*N*-diethyl-β,γ-dibromomethylene-D-ATP, cat no. A265), the adenosine 5′-trisphosphate (ATP) assay mix (FLAAM), ATP, and LY were obtained from Sigma-Aldrich. Gap26 peptide (VCYDKSFPISHVR) was synthesized (Milligen 9050; PepSynthesizer, Applied Biosystems, Inc., Foster City, CA) at the Laboratory of Biochemistry, Katholieke Universiteit, Leuven. The peptides were routinely analyzed by reversed-phase HPLC (Waters Corp., Milford, MA), on a C18-column (250 × 4.60 mm); Luna 5u, Phenomenex, Torrance, CA) using a linear gradient of acetonitrile–water, containing 0.06% trifluoroacetic acid (TFA). The exact sequence of the peptide was confirmed by electrospray ionization (ESI)-triple quadrupole mass spectrometry (API-3000 mass spectrometer; MDS Sciex, Applied Biosystems, Inc.). The purity of the peptide was greater than 95%.

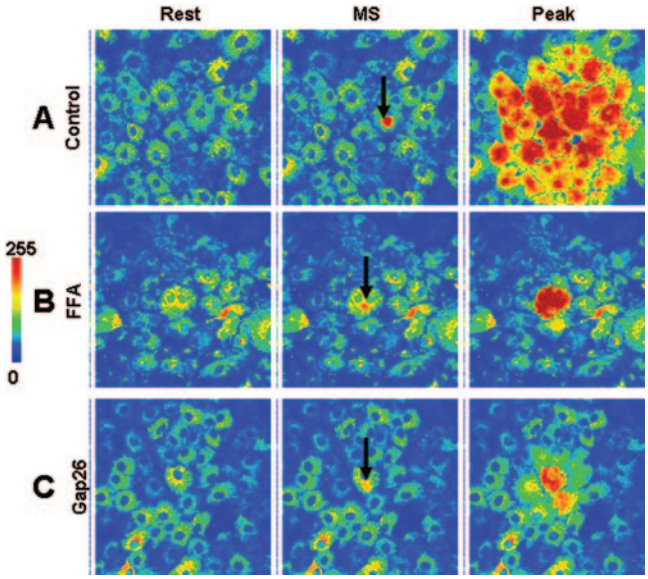

FIGURE 1. FFA and Gap26 inhibit intercellular Ca^{2+} wave propagation in BCECs. Shown are pseudocolored fluorescence images of cells loaded with Fluo-4 AM, before (*left*), immediately after mechanical stimulation of a single cell (*middle*) and at the time of peak response (*right*) in control conditions (*top row*) and in cells treated with 50 μM FFA (*middle row*) or 300 μM Gap26 (*bottom row*) for 30 minutes. *Arrows*: MS cell. The color scale at *left* represents the changes in fluorescence induced by the $[Ca^{2+}]_i$ changes.

Data Analysis

All data are given as the mean ± SEM. Comparisons of means between groups were performed by unpaired *t*-tests, with $P < 0.05$ considered a statistically significant difference. *N* indicates the number of independent experiments (equal to number of cells subjected to PMS), whereas *n* represents the total number of cells.

RESULTS

Effect of FFA and Gap26 on the Ca^{2+} Wave Propagation

Our previous work showed that PMS-induced intercellular Ca^{2+} wave propagation in BCECs is partially mediated by ATP release into the extracellular space.[4] Because it has been suggested that hemichannels may play a role in ATP release[34,42] and because the presence of connexin (Cx)43 has been demonstrated in BCECs,[43] we investigated whether hemichannels are involved in PMS-induced Ca^{2+} wave propagation in BCECs. We began by examining the effect of putative hemichannel blockers on the intercellular Ca^{2+} wave propagation. Figure 1 shows that the spread of the PMS-induced Ca^{2+} wave was strongly inhibited by FFA (50 μM) and by Gap26 (300 μM) (a connexin-mimetic peptide specific for Cx43). The NF in the NB cells, %RC, and the AA were significantly reduced by FFA or Gap26, as shown in Figure 2 and summarized in Table 1. Furthermore, the inhibition of the wave propagation by FFA is greater than the inhibition caused by the addition of Gap26.

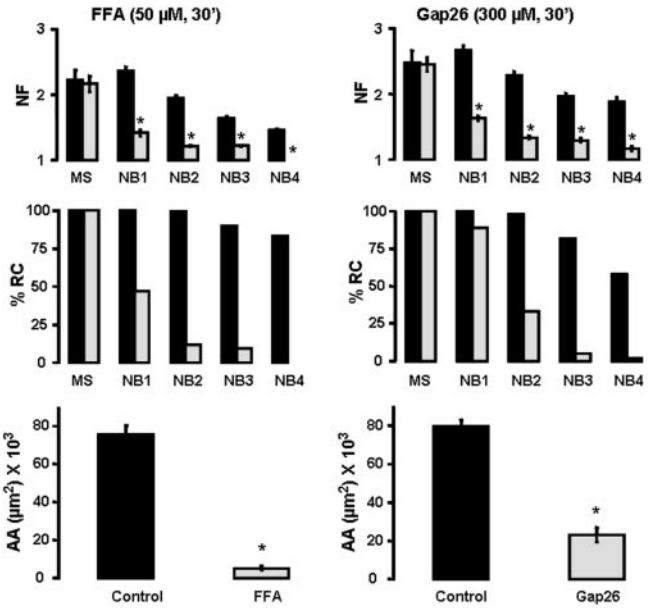

FIGURE 2. Inhibition of Ca^{2+} wave propagation in BCECs by FFA and Gap26. The data show the effect of a 30-minute application of 50 μM FFA (*left*) or 300 μM Gap26 (*right*) on the maximum NF, the %RC, and AA of Ca^{2+} wave propagation in response to PMS. (■) Control; (▨) drug. *Significant difference at $P < 0.05$ vs. control.

Lack of Effect of FFA and Gap26 on Gap Junctional Intercellular Communication

Because the PMS-induced Ca^{2+} wave propagation in BCECs is only partially mediated through the purinergic pathway,[4] it is likely that gap junctional intercellular communication (GJIC) also plays a role. We therefore wanted to verify that the effect of the putative hemichannel blockers was not due to inhibition of GJIC. Accordingly, we performed FRAP experiments using carboxyfluorescein (a dye known to permeate gap junctions) in the presence of hemichannel blockers. The percentages of fluorescence recovery at 3 minutes in the presence of FFA (63.09% ± 2.43%, $N = 54$) or Gap26 (64.93% ± 1.71%, $N = 63$) were not significantly different from the control (65.88% ± 1.36%, $N = 90$). These data indicate that FFA or Gap26 have no effect on gap junctional coupling and hence that their inhibition of the spread of the PMS-induced Ca^{2+} wave is not due to the blocking of gap junctions.

Effect of FFA and Gap26 on Paracrine Intercellular Communication

Application of the ectonucleotidase inhibitor ARL-67156 caused a marked enhancement of the spread of the Ca^{2+} wave propagation in BCECs via a paracrine intercellular communication (PIC) pathway, presumably by increasing the availability of the putative paracrine factor ATP.[4] To study whether the release of the paracrine factor is mediated through hemichannels, we investigated whether the enhancement of the Ca^{2+} wave induced by ARL-67156 (100 μM) was affected by application of FFA or Gap26. The results are summarized in Figure 3. The AA was 149,648 ± 25,273 μm^2 ($N = 12$) in control conditions and increased to 544,605 ± 32,183 μm^2 ($N = 17$) in cells pretreated with ARL-67156 for 30 minutes, indicating that ATP hydrolysis limits the PMS-induced Ca^{2+} wave propagation. However, when cells were pre-exposed for 30 minutes to a combination of ARL-67156 and FFA or ARL-67156 and Gap26, the AAs were only 30,788 ± 4,675 μm^2 ($N = 20$) and 103,756 ± 10,329 μm^2 ($N = 18$), respectively. The very large enhancement of the wave by ARL-67156 was blocked by FFA and Gap26. This finding strongly suggests that both FFA and Gap26 act by limiting the amount of substrate available for the ectonucleotidases, presumably by limiting the release of the paracrine factor involved in intercellular propagation of the Ca^{2+} wave in BCECs.

Previous experiments in which cells were scraped out in a confluent monolayer to make a cell-free lane showed that a Ca^{2+} rise elicited by PMS spread out not only to the NB cells on the MS side, but also to the NB cells across the cell-free lane. Furthermore, the propagation of the Ca^{2+} wave across the cell-free lane was enhanced on pretreatment with ARL-67156.[4] To obtain further evidence that FFA and Gap26 inhibit the release of the paracrine factor involved in the spread of the PMS-induced Ca^{2+} wave, we examined their efficacy in inhibiting the propagation of the wave across cell-free lanes, a

TABLE 1. Average Maximum NF, %RC, and AA, in the MS and NB Cells during Mechanical Stimulation in Control Conditions and after Treatment with FFA or Gap26

	MS	NB1	NB2	NB3	NB4	AA (μm^2)
Control for FFA						75,466 ± 4,932
NF	2.22	2.36	1.95	1.64	1.45	
SEM	0.15	0.06	0.03	0.03	0.02	
n	24	140	281	321	216	
%RC	100	100	99	90	83	
FFA (50 μM)						5,272 ± 1,060*
NF	2.16	1.42*	1.21*	1.22*	0.00*	
SEM	0.12	0.05	0.01	0.01	0.00	
n	15	92	180	200	112	
%RC	100	47	12	9	0	
Control for Gap26						79,496 ± 3,465
NF	2.48	2.66	2.28	1.96	1.88	
SEM	0.19	0.08	0.06	0.05	0.07	
n	16	114	224	289	189	
%RC	100	100	98	81	58	
Gap26 (300 μM)						23,123 ± 3,856*
NF	2.45	1.63*	1.33*	1.29*	1.16*	
SEM	0.11	0.04	0.02	0.03	0.03	
n	19	124	244	314	221	
%RC	100	89	33	5	2	

* $P < 0.05$ vs. control.

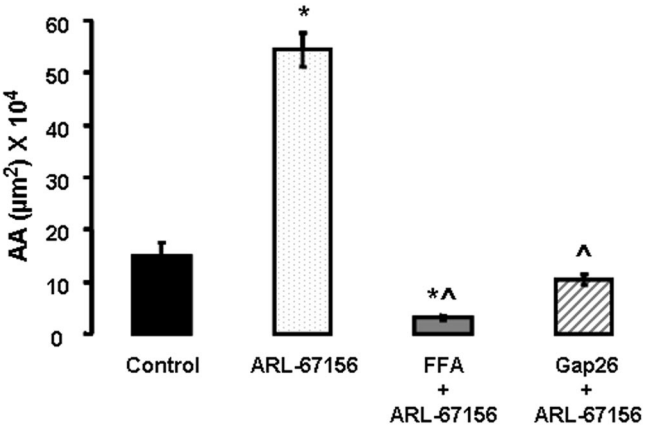

FIGURE 3. FFA and Gap26 inhibited Ca^{2+} wave propagation in BCECs via the PIC pathway. The ectonucleotidase inhibitor ARL-67156 (100 μM) caused a large increase of the active area (AA) of Ca^{2+} wave propagation. The effect of ARL-67156 was inhibited by blocking hemichannels with either FFA (50 μM) or Gap26 (300 μM). $^*P < 0.05$ versus control. $^\wedge P < 0.05$ versus ARL-67156.

condition that excludes a role of GJIC. On pretreatment of the cells with FFA (50 μM) or Gap26 (300 μM), the spread of the Ca^{2+} wave was reduced on the MS side when compared to control conditions, whereas it was completely abolished across the cell-free lane. On pretreatment with a combination of ARL-67156 and FFA or a combination of ARL-67156 and Gap26 for 30 minutes, the enhancement of the spread of the Ca^{2+} wave due to ARL-67156 was also totally abolished (Fig. 4). However, in the presence of either FFA or Gap26, ARL-67156 still had a strong effect on the MS side as well as on the other side when compared with FFA or Gap26 alone, providing evidence that the effect of ARL-67156 on the ectonucleotidases is not lost (Fig. 4).

These results provide further evidence that the effects of the hemichannel blockers FFA or Gap26 are exerted via the PIC pathway and further substantiate the hypothesis that the effects of FFA and Gap26 are due to the inhibition of ATP release via hemichannels.

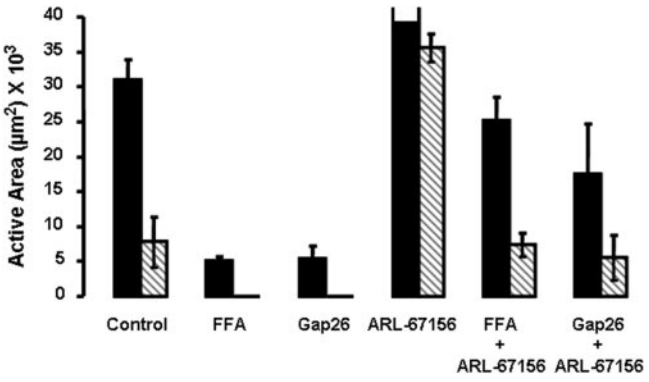

FIGURE 4. FFA and Gap26 inhibited Ca^{2+} wave propagation across cell-free lanes. Data represent the AA after PMS on both sides of a cell-free lane. Results are from five experiments in each of the different conditions. (■) AA on the side of PMS; (▨) AA on the other side of the cell-free lane. FFA (50 μM) or Gap26 (300 μM) blocked the spread of the Ca^{2+} wave across cell-free lanes. The large increase of the spread of the Ca^{2+} wave across the cell-free lane by 100 μM ARL-67156 in control conditions was largely inhibited by FFA or Gap26. Because in the presence of ARL-67156 the AA exceeded the size of the image on the side of the PMS, this value is represented by an *open-ended solid bar*.

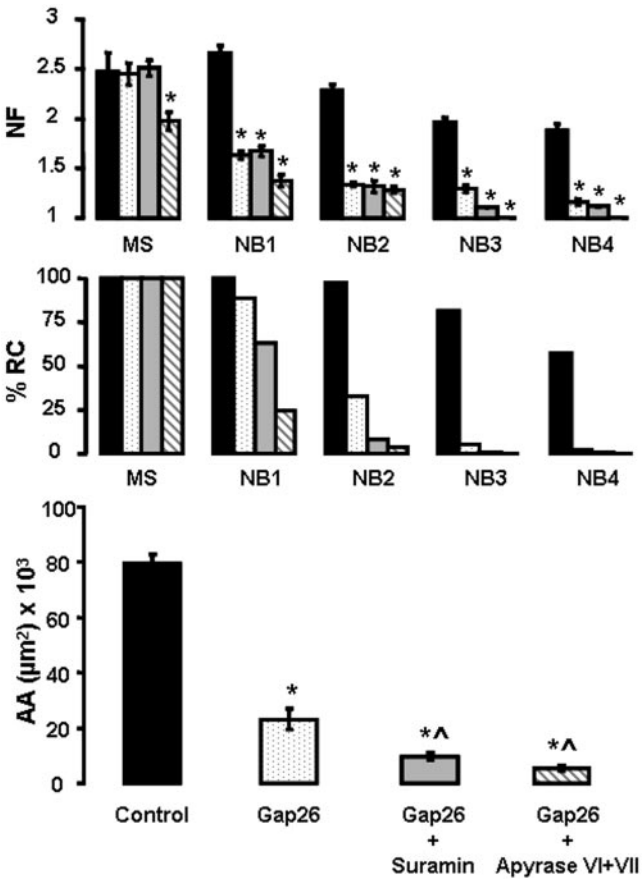

FIGURE 5. Effect of suramin or apyrase in the presence of Gap26. Cells were treated for 30 minutes with Gap26, Gap26+apyrase VI+VII, or Gap26+suramin. The Ca^{2+} wave propagation in response to PMS is represented in control (■; $N = 16$), Gap26 (▨; $N = 19$), Gap26+suramin (■; $N = 18$), or Gap26+apyrase VI+VII (▨; $N = 18$). *Top*: maximum normalized fluorescence (NF); *middle*: %RC for MS and NB1 to NB4; *bottom*: AA for the different experimental conditions. Concentrations: Gap26 (300 μM), apyrase VI+VII (5 U/mL each), suramin (200 μM). $^*P < 0.05$ versus control. $^\wedge P < 0.05$ versus Gap26.

To exclude that the inhibitory effects of FFA or Gap26 on Ca^{2+} wave propagation are due to direct effects on P2Y receptors or due to the depletion of intracellular Ca^{2+} stores, we exposed cells pre-treated with 50 μM FFA (NF: 1.9 ± 0.1, $N = 4$) or 300 μM Gap26 (NF: 1.8 ± 0.1, $N = 4$) to 100 μM ATP. In these conditions the NF of the cells was not significantly different when compared to application of 100 μM ATP in control conditions for FFA (1.97 ± 0.24, $N = 4$) or control conditions for Gap 26 (2.0 ± 0.09, $N = 4$).

To find out how much of the PIC component was being inhibited by blocking hemichannels, we studied the effect of PIC blockers on the Ca^{2+} wave in the presence of Gap26. The results showed that the combination of the PIC inhibitors (200 μM suramin or apyrase VI+apyrase VII (5 U/mL each); see[4]) with Gap26 (300 μM) caused a small further reduction of the Ca^{2+} wave when compared to Gap26 (Fig. 5 and Table 2).

Effect of FFA or Gap26 on Hemichannels

To show that FFA- and Gap26-induced inhibition of the spread of the PMS-induced Ca^{2+} wave is through a block of the hemichannels, we investigated the effects of the agents on hemichannels. Because hemichannels are known to open in conditions of low extracellular Ca^{2+}, and the resulting opened channels are permeable to several hydrophilic solutes, includ-

TABLE 2. Average NF, %RC, and AA in the MS and NB Cells during Mechanical Stimulation in Control Conditions and in Cells Treated with Gap26, Gap26+suramin, or Gap26+apyrase VI + VII

	MS	NB1	NB2	NB3	NB4	AA (μm^2)
Control						79,496 ± 3,465
NF	2.48	2.66	2.28	1.96	1.88	
SEM	0.19	0.08	0.06	0.05	0.07	
n	16	114	224	289	189	
%RC	100	100	98	81	58	
Gap26 (300 μM)						23,123 ± 3,856*
NF	2.45	1.63*	1.33*	1.29*	1.16*	
SEM	0.11	0.04	0.02	0.03	0.03	
n	19	124	244	314	221	
%RC	100	89	33	5	2	
Gap26 (300 μM) + suramin (200 μM)						9,598 ± 1,414*
NF	2.51	1.67*	1.32*	1.10*	1.12*	
SEM	0.08	0.05	0.06	0.00	0.00	
n	18	111	242	311	208	
%RC	100	63	8	1	1	
Gap26 (300 μM) + apyrase VI + VII (5 U/mL each)						5,343 ± 912*
NF	1.98*	1.37*	1.28*	0.00*	0.00*	
SEM	0.09	0.06	0.03	0.00	0.00	
n	18	123	234	291	180	
%RC	100	24	3	0	0	

The combination of the PIC inhibitors (200 μM suramin or apyrase VI + apyrase VII [5 U/mL each]) with 300 μM Gap26 resulted in a further reduction of the Ca^{2+} wave when compared to Gap26 alone.

* $P < 0.05$ vs. control.

ing ATP and LY,[44,45] we exposed a subconfluent monolayer of BCECs to LY in the presence and absence of extracellular Ca^{2+} (Fig. 6). In the presence of extracellular Ca^{2+} (1.5 mM) none of the cells showed uptake of dye after 5 minutes of exposure to the dye ($N = 20$). In contrast, exposure to Ca^{2+}-free solutions containing EGTA (2 mM) led to significant uptake of the dye by all cells ($N = 24$). However, when cells pretreated for 30 minutes with FFA ($N = 20$) or Gap26 ($N = 20$) were exposed to Ca^{2+}-free conditions, no uptake of LY was observed (Fig. 6). These observations, taken together, indicate that BCECs possess hemichannels which open in Ca^{2+}-free solutions, and most important, the opened hemichannels are blocked by FFA and Gap26.

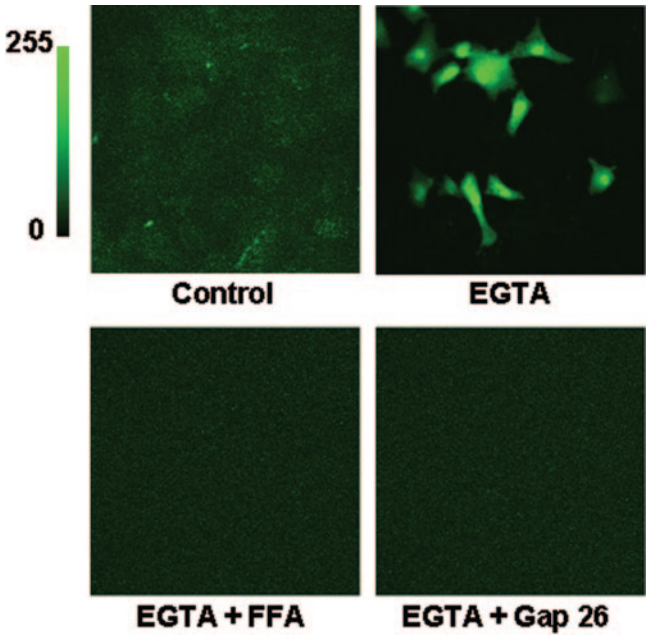

FIGURE 6. Uptake of LY in Ca^{2+}-free solutions was inhibited by FFA and Gap26. Cells were exposed to the fluorescent dye LY for 5 minutes in the presence and absence of extracellular Ca^{2+}. The uptake of the dye in Ca^{2+}-free conditions (2 mM EGTA) was blocked in cells pretreated for 30 minutes with 50 μM FFA or 300 μM Gap26.

Effect of Ca^{2+}-Free Solution on ATP Release

Because Stout et al.[34] have shown that hemichannels open on exposure to low extracellular Ca^{2+} and show permeability to ATP and several hydrophilic dyes such as LY, we tested the hypothesis that hemichannels opened by Ca^{2+}-free solutions in BCECs also release ATP.[34,46] Results of a typical experiment showing ATP release versus time are presented in Figure 7. The peak height of the first transient (labeled 0) in response to an

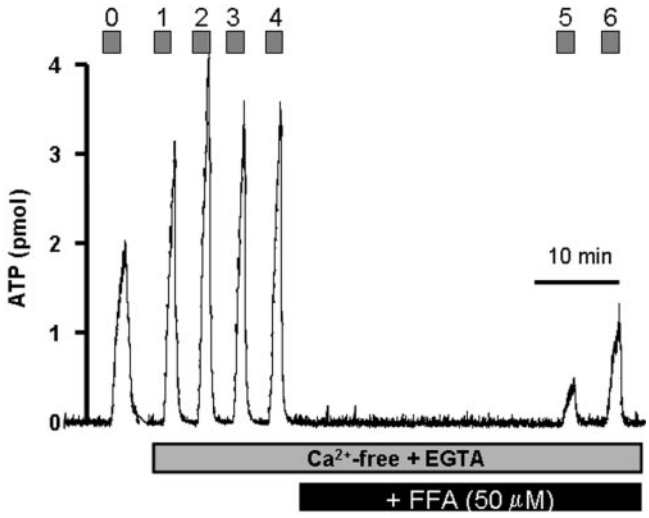

FIGURE 7. ATP release in Ca^{2+}-free conditions was inhibited by FFA. Shown is the measurement of extracellular ATP with the LL technique during perfusion experiments on BCECs. The *squares* above the peaks numbered 0 to 6 represent application of LL during the experiment. The LL pulse 0: the ATP measurement in control conditions; 1 to 4: on exposure to 2 mM EGTA; 5 and 6: ATP measurements on treatment with 50 μM FFA.

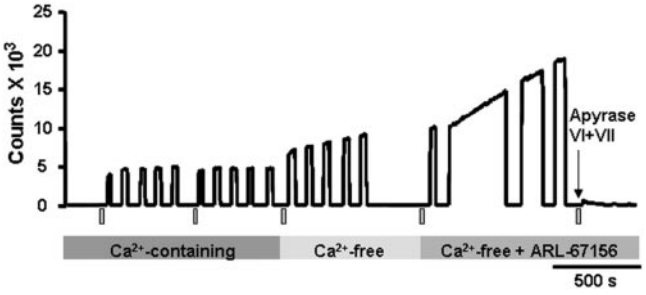

FIGURE 8. ATP released in Ca^{2+}-free conditions was enhanced in the presence of ARL-67156. Shown is the measurement of extracellular ATP using the LL technique in experiments on BCECs with intermittent renewal of bathing solution. The *narrow rectangles* below the peaks represent points of renewal of the bathing solution, together with application of LL. After every renewal, the shutter of the photon counter was temporarily opened to measure the ATP counts at different time points. Application of Ca^{2+}-free solution containing 2 mM EGTA enhanced the ATP-luminescence counts. These counts were further enhanced in the presence of 100 μM ARL-67156. Application of apyrase VI+VII (5 U/mL each) at the end of the experiment almost completely abolished the ATP counts.

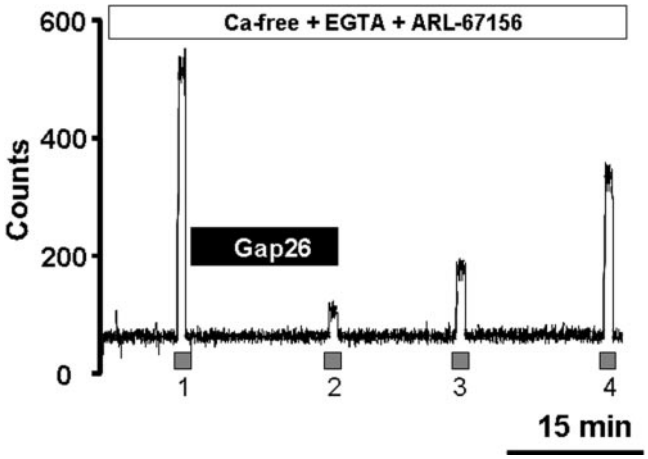

FIGURE 9. ATP release in Ca^{2+}-free conditions was reversibly inhibited by Gap26. Shown are luminescence counts for ATP in Ca^{2+}-free conditions. ARL-67156 (100 μM) was applied to prevent ATP breakdown by ectonucleotidases. Measurements were performed with intermittent renewal of the bathing solution. The *squares* below the transients represent the renewal of the bathing solution along with application of LL.

LL pulse represents the amount of ATP accumulated during 1.5 minutes in Ca^{2+}-containing solution. The peak heights of the subsequent transients (labeled 1, 2, 3, and 4) in response to LL pulses correspond to ATP released under Ca^{2+}-free conditions. These experiments clearly demonstrate that the ATP release (presumably through opening of hemichannels) was markedly increased in Ca^{2+}-free solution.

Because we knew from previous experiments that the ectonucleotidase inhibitor ARL-67156 enhances PIC in BCECs,[4] we next studied the effects of the inhibitor on the ATP released in Ca^{2+}-free solutions in experiments with the setup for intermittent renewal of solution (see the Materials and Methods section). Exposure of cells to ARL-67156 strongly enhanced the amount of extracellular ATP when compared with control conditions (Fig. 8). Application of apyrase VI+VII (5 U/mL each) at the end of the experiment almost completely abolished the extracellular ATP.

Effect of Hemichannel Blockers on ATP Release in Ca^{2+}-Free Solution

We next investigated whether the release of ATP in the absence of extracellular Ca^{2+} is blocked by hemichannel blockers. We therefore measured ATP release in cells treated with FFA. As shown by the transients labeled 5 and 6 in Figure 7, the increase of ATP release in Ca^{2+}-free solutions was inhibited by exposing the cells to FFA for 30 minutes. Similar results were obtained in four independent experiments. We also investigated whether Gap26 inhibits release of ATP. To limit consumption of Gap26, the effect of the peptide was examined in experiments with intermittent renewal of solution (see the Material and Methods section). These experiments were performed in the presence of 100 μM ARL-67156, to inhibit the hydrolysis of ATP by ecto-ATPases. Results showed that also 300 μM Gap26 (30 minutes) strongly decreased the luminescence counts when compared with control conditions and that this inhibitory effect was reversed on washing out Gap26 (Fig. 9). These experiments show that BCECs possess hemichannels that release ATP and that can be blocked by FFA or Gap26.

ATP Release during PMS

The involvement of ATP release in the Ca^{2+} wave propagation, as suggested by the inhibition of the Ca^{2+} wave in the presence of the hemichannel blockers, was further investigated by direct measurement of ATP release in response to PMS. Cells were subjected to PMS as in Ca^{2+} wave experiments. At various time points before and after application of a PMS, the bathing fluid was sampled for ATP (see the Materials and Methods section). PMS led to a 1.5- to 2-fold increase in ATP release (transient 2 in Fig. 10) relative to basal conditions (transients 0 and 1, Fig. 10). Similar results were obtained in all 15 independent experiments. The level of ATP in the bath gradually declined with time after PMS (transients 3 and 4, Fig. 10), which is presumably due to the activity of ectonucleotidases. Accordingly, application of ARL-67156 enhanced the basal ATP level (transients 5 and 6, Fig. 10). In the presence of ARL-67156, PMS produced a larger increase in ATP (transient 7, Fig. 10), and the ATP level in the bath continued to increase with time, consistent with the continuous basal release of ATP, which can accumulate in the bath as a result of inhibition of ecto-nucleotidases.

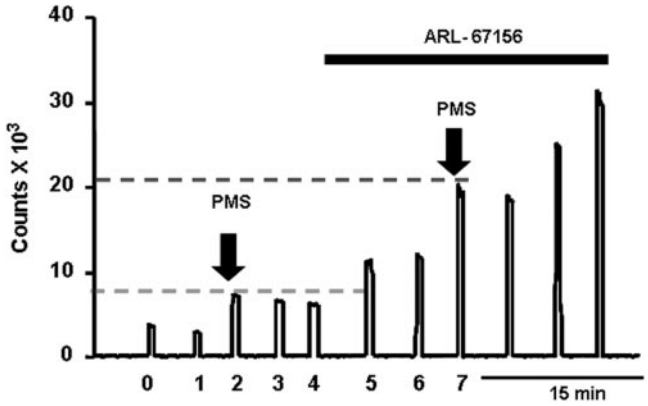

FIGURE 10. ATP release increased in response to PMS. Shown are luminescence counts for ATP in Ca^{2+}-containing conditions in samples of 25 μL taken from the bathing solution. *Arrows*: measurement of ATP in samples taken immediately after PMS. The peaks labeled 0 and 1 show the basal ATP release. The luminescence increased on PMS (2) and slowly decreased with time (3 and 4). Exposure to ARL-67156 (100 μM) increased the amount of ATP in the bath (5 and 6). PMS in the presence of ARL-67156 caused a further increase in luminescence (7). Afterward, a gradual luminescence increase was observed.

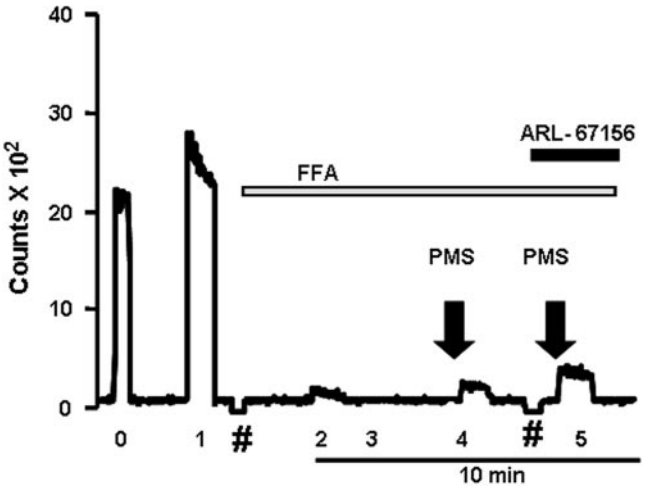

FIGURE 11. The increase of extracellular ATP in response to PMS was inhibited by FFA. Shown are luminescence counts for ATP in Ca^{2+}-containing conditions in samples of 25 μL taken from the bathing solution. Peaks 0 and 1 show luminescence counts due to basal ATP release. After treatment with 50 μM FFA for 30 minutes the basal luminescence counts were almost abolished (2 and 3). PMS in FFA caused a slight, nonsignificant increase (4). Exposure to ARL-67156 (100 μM) for 30 minutes did not significantly increase the counts (5). #Points of replacement of bathing solution and treatment with FFA or ARL-67156.

Effect of Hemichannel Blockers on PMS-Induced ATP Release

The PMS-induced ATP release was also significantly inhibited at all time points of sampling by both FFA and Gap26 (Figs. 11, 12, respectively) even in the presence of ARL-67156. Experiments were repeated four times, and all trials gave similar results.

DISCUSSION

Exposure to acute hyposmotic stress or mechanical stimuli results in a release of intracellular ATP leading to autocrine–paracrine effects, and therefore is reported to have attendant pathophysiological implications.[47–51] Although ATP release has now been demonstrated in a large number of cell types, the pathway(s) of the release has been very controversial.[52–54] ATP, being a charged molecule at physiological pH, requires a vesicular process and/or an (ATP^{4-})-permeable channel for its efflux. In this study, we examined connexin hemichannels as a candidate pathway for ATP release and its influence on PMS-induced Ca^{2+} wave propagation in corneal endothelial cells. Our key findings include: (1) ATP release and uptake of LY induced by removal of extracellular Ca^{2+} were inhibited by the recently identified blockers of hemichannels: FFA and Gap26, (2) PMS-induced Ca^{2+} wave propagation, which was shown to be dependent on ATP release and subsequent activation of purinergic receptors on the NB cells,[4] was inhibited by FFA and Gap26, and (3) PMS induced ATP release, which is also inhibited by FFA and Gap26. These results suggest that hemichannels form a pathway for ATP release in BCECs that contributes to the Ca^{2+} wave propagation elicited by PMS. This conclusion is similar to the findings by Stout et al.[34] and Leybaert et al.[35,42] in astrocytes.

Specific blockers for hemichannels are not yet known. Therefore, a panel of inhibitors is usually used to show their involvement in any given physiological function. In this study, we initially contemplated using Gd^{3+}, in addition to FFA and Gap26, to investigate the involvement of hemichannels in ATP release by two different types of measurements: PMS-induced ATP release (using LL bioluminescence) and Ca^{2+} wave propagation (detected by $[Ca^{2+}]_i$ imaging). The bioluminescence assay, which is reported to be sensitive to Gd^{3+}, was unaffected by Gap26 (see the Materials and Methods section). Furthermore, because Gd^{3+} can bind to certain anions including ATP, stimulate ATP efflux, inhibit capacitative Ca^{2+} entry pathways, and block stretch-activated cation channels, we excluded its use in our studies.[55]

The efficacy of FFA and Gap26 was also confirmed with a permeability assay for hemichannels. Removal of extracellular Ca^{2+} induced uptake of LY (Fig. 6), which was completely inhibited by FFA and Gap26. These observations suggest that hemichannels are present in BCECs and can be blocked by FFA and Gap26. The underlying assumption that the removal of extracellular Ca^{2+} leads to opening of hemichannels is further supported by the immediate increase in the rate of ATP release, as shown in Figure 7. Similar to the dye uptake, both FFA and Gap26 also inhibited ATP release, indicating that both agents inhibit the release by the same mechanism. This interpretation is supported by the fact that, in astrocytes, ATP release and permeability to low-molecular-weight dyes have a similar Ca^{2+}-dependency.[56] A candidate molecule that permits permeation of hydrophilic membrane-impermeable dyes (such as LY) is the ATP-gated ion channel, P2X7 receptors.[57–61] However, functional P2X7 receptors are not found in BCECs.[14,62]

Apart from the fact that both FFA and Gap26 showed significant inhibition of dye uptake and ATP release, we could not glean much about the mechanism of the inhibition. However, it is worth noting that FFA is a known Cl^- channel blocker. Based on the large anionic conductance in resting conditions and the nature of the electrochemical gradient ($[Cl^-]_i \sim -35$ mM and resting $E_m \sim -50$ mV in the absence of HCO_3^-; see Ref. 63) in corneal endothelial cells, nonspecific Cl^- channel blockade is likely to hyperpolarize the membrane potential, which might, in turn, inhibit GJIC and hemichannels; but the same cannot be said about the inhibition by Gap26. It is a connexin-mimetic peptide with sequence similarity to the

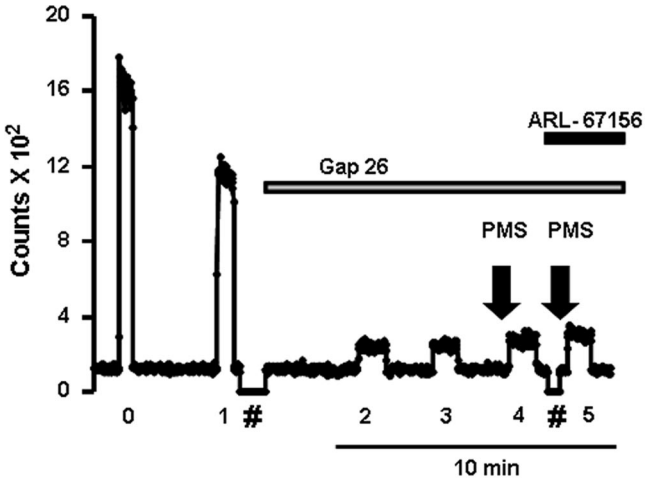

FIGURE 12. The increase of extracellular ATP in response to PMS was inhibited by Gap26. Shown are luminescence counts for ATP in Ca^{2+}-containing conditions in samples of 25 μL taken from the bathing solution. The peaks labeled 0 and 1 show the basal ATP release. After treatment with 300 μM Gap26 for 30 minutes, the basal ATP counts were strongly inhibited (2 and 3). PMS in Gap26 caused an insignificant increase (4). Exposure to ARL-67156 (100 μM) for 30 minutes did not significantly increase the counts (5). #Points of replacement of the bathing solutions and treatment with Gap26 or ARL-67156 for 30 minutes.

E1 subdomain (extracellular domain of the first transmembrane loop) of Cx43.[64] Gap26-mediated inhibition is relatively selective for hemichannels with Cx43 isoforms of connexins,[42] which are expressed in bovine[43] and human[65] corneal endothelium.

It is readily apparent in Figures 1 and 2 and Table 1 that both FFA and Gap26 significantly inhibited the PMS-induced Ca^{2+} wave propagation. Although our previous study ascertained that extracellular ATP contributes to the wave propagation in BCECs, it does not exclude an eventual contribution of a gap junctional pathway.[4] The role of extracellular ATP had been ascertained by showing partial inhibition of the wave by P2Y antagonist and exogenous apyrases and most readily by the spread of the wave across isolated cells lacking gap junctions. The inhibition of the Ca^{2+} wave propagation, shown in Figures 1 and 2, and Table 1 is therefore suggestive of one or more of the following mechanisms: (1) blocking of PMS-induced ATP release by FFA and Gap26, (2) blocking of gap junctions by FFA and Gap26, (3) antagonism of the P2Y or IP_3 receptors, and/or (4) direct toxicity to cells. We rule out direct antagonism of P2Y receptors and IP_3 receptors or toxicity, since, in the presence of FFA or Gap26, application of exogenous ATP induced the increase of $[Ca^{2+}]_i$, as in control conditions. We cannot attribute the inhibition of the wave to a block of the gap junctions, because neither FFA nor Gap26 affected the extent of recovery of fluorescence in the FRAP experiments. Thus, we are left with the only possibility: that the blockers directly act on the mechanism of ATP release after PMS. This notion was confirmed by direct measurement of ATP in samples of the bathing fluid immediately after PMS. In several independent trials, both Gap26 and FFA inhibited ATP release. Both agents also inhibited the release of ATP in basal conditions.

In many cell types, such as neurons, astrocytes, MDCK-D_1 cells, or platelets, two forms of ATP release have been reported.[66,67] First, intact cells constitutively release ATP, albeit at low rates, in the absence of lysis or loss of plasma membrane integrity.[68] Second, the rate of nonlytic ATP release can be greatly increased by a variety of external stimuli that result in perturbation of cell volume, shape, cytoskeletal organization, or intracellular Ca^{2+} homeostasis. In agreement with these studies, we demonstrated that a basal (or "constitutive") release of ATP is a characteristic of BCECs and that ATP release can be enhanced by removal of extracellular Ca^{2+} or by PMS. The measured extracellular ATP concentrations reflect the balance between the cellular release of ATP and the efficiency of their ATP-hydrolyzing ectoenzymes and eventual transphosphorylating activity of extracellular forms of nucleotide diphosphokinase or adenylate kinase.[68] They are, however, unlikely to reflect accurately the concentration at the cell surface and reflect probably only a fraction of the actual nucleotide concentration that is present in the vicinity of the P2Y receptors.[68,69]

While our results demonstrate that PMS of BCECs induced ATP release through hemichannels, we cannot exclude that other mechanisms also contributed to the ATP release via such pathways as exocytosis[52,70–72] of ABC proteins such as P-glycoprotein and CFTR,[73,74] and other anion transporters[72] and Cl^- channels[29] such as the voltage-dependent[75] and -independent[76] volume-regulated anion channels (VRACs). Recently, pannexins have been proposed as potential candidates for ATP release.[77] Pannexin 1 is widely distributed among tissues with cell communication via calcium waves.[77] The channel formed by this protein can be opened by mechanical perturbation at the resting membrane potential.[78] The channel is permeable to ATP and can be opened at the physiological calcium concentration.[77]

Hemichannels, per se, have not been examined to date in the corneal endothelium. In fact, little has been reported on gap junctions and their physiological role in the corneal endothelium. However, the expression of Cx43 (as shown by immunocytochemistry) has been demonstrated in BCECs.[43] Moreover, expression of Cx43 and gap junctional dye coupling have been reported in human corneal endothelial cells.[65] Given this background, this is the first study involving hemichannels in the corneal endothelium. In addition to the role of ATP release in promoting intercellular communication (as exemplified by Ca^{2+} wave propagation in this study), hemichannels can be expected to possess other physiological functions. In this regard, it is important to recall that the hemichannels open in response to metabolic ATP depletion.[79] This may have two important consequences in the corneal endothelium: (1) accelerated ATP depletion leading to cell death, and (2) cell swelling as a consequence of hemichannel-mediated influx of cations. The former may contribute to the observed polymegathism and polymorphism that is known to occur after corneal hypoxia, presumably due to cell death as a result of ATP depletion. Because the endothelial cells are nonregenerative, the denuded areas left by loss of cells (by apoptosis or necrosis) are covered by cell spreading, leading to polymegathism and polymorphism.

In conclusion, we demonstrated that functional hemichannels are found in BCECs, which are opened by low extracellular Ca^{2+} and in response to mechanical stimulation, and that ATP release through hemichannels contributes to PMS-induced intercellular Ca^{2+} wave propagation.

References

1. Cotrina ML, Lin JH, Lopez-Garcia JC, et al. ATP-mediated glia signaling. *J Neurosci*. 2000;20:2835–2844.
2. Braet K, Paemeleire K, D'Herde K, et al. Astrocyte-endothelial cell calcium signals conveyed by two signalling pathways. *Eur J Neurosci*. 2001;13:79–91.
3. Himpens B, Stalmans P, Gomez P, et al. Intra- and intercellular Ca^{2+} signaling in retinal pigment epithelial cells during mechanical stimulation. *FASEB J*. 1999;13:S63–S68.
4. Gomes P, Srinivas SP, Vereecke J, Himpens B. ATP-dependent paracrine intercellular communication in cultured bovine corneal endothelial cells. *Invest Ophthalmol Vis Sci.* 2005;46:104–113.
5. Charles AC, Merrill JE, Dirksen ER, Sanderson MJ. Intercellular signaling in glial cells: calcium waves and oscillations in response to mechanical stimulation and glutamate. *Neuron*. 1991;6:983–992.
6. Paemeleire K, Leybaert L. ATP-dependent astrocyte-endothelial calcium signaling following mechanical damage to a single astrocyte in astrocyte-endothelial co-cultures. *J Neurotrauma*. 2000;17:345–358.
7. Frame MK, de Feijter AW. Propagation of mechanically induced intercellular calcium waves via gap junctions and ATP receptors in rat liver epithelial cells. *Exp Cell Res*. 1997;230:197–207.
8. Sanderson MJ. Intercellular calcium waves mediated by inositol trisphosphate. *Ciba Found Symp*. 1995;188:175–189.
9. Moerenhout M, Himpens B, Vereecke J. Intercellular communication upon mechanical stimulation of CPAE-endothelial cells is mediated by nucleotides. *Cell Calcium*. 2001;29:125–136.
10. Zhang Y, Xie Q, Sun XC, Bonanno JA. Enhancement of HCO_3^- permeability across the apical membrane of bovine corneal endothelium by multiple signaling pathways. *Invest Ophthalmol Vis Sci*. 2002;43:1146–1153.
11. Boland B, Himpens B, Vincent MF, et al. ATP activates P2x-contracting and P2y-relaxing purinoceptors in the smooth muscle of mouse vas deferens. *Br J Pharmacol*. 1992;107:1152–1158.
12. Riley MV, Winkler BS, Starnes CA, et al. Regulation of corneal endothelial barrier function by adenosine, cyclic AMP, and protein kinases. *Invest Ophthalmol Vis Sci*. 1998;39:2076–2084.
13. Bonanno JA. Identity and regulation of ion transport mechanisms in the corneal endothelium. *Prog Retin Eye Res*. 2003;22:69–94.

14. Srinivas SP, Yeh JC, Ong A, Bonanno JA. Ca^{2+} mobilization in bovine corneal endothelial cells by P2 purinergic receptors. *Curr Eye Res*. 1998;17:994–1004.
15. Okada Y, Maeno E, Shimizu T, et al. Receptor-mediated control of regulatory volume decrease (RVD) and apoptotic volume decrease (AVD). *J Physiol*. 2001;532:3–16.
16. Morrone FB, Jacques-Silva MC, Horn AP, et al. Extracellular nucleotides and nucleosides induce proliferation and increase nucleoside transport in human glioma cell lines. *J Neurooncol*. 2003;64:211–218.
17. Cha SH, Hahn TW, Sekine T, et al. Purinoceptor-mediated calcium mobilization and cellular proliferation in cultured bovine corneal endothelial cells. *Jpn J Pharmacol*. 2000;82:181–187.
18. Burnstock G. Purinergic signaling and vascular cell proliferation and death. *Arterioscler Thromb Vasc Biol*. 2002;22:364–373.
19. Greig AV, Linge C, Terenghi G, et al. Purinergic receptors are part of a functional signaling system for proliferation and differentiation of human epidermal keratinocytes. *J Invest Dermatol*. 2003;120:1007–1015.
20. Illes P, Alexandre Ribeiro J. Molecular physiology of P2 receptors in the central nervous system. *Eur J Pharmacol*. 2004;483:5–17.
21. Dell'Antonio G, Quattrini A, Cin ED, et al. Relief of inflammatory pain in rats by local use of the selective P2X7 ATP receptor inhibitor, oxidized ATP. *Arthritis Rheum*. 2002;46:3378–3385.
22. Dubyak GR, el-Moatassim C. Signal transduction via P2-purinergic receptors for extracellular ATP and other nucleotides. *Am J Physiol*. 1993;265:C577–C606.
23. Brake AJ, Julius D. Signaling by extracellular nucleotides. *Annu Rev Cell Dev Biol*. 1996;12:519–541.
24. Forrester T. A quantitative estimation of adenosine triphosphate released from human forearm muscle during sustained exercise. *J Physiol.* 1972;221:25P–26P.
25. Bodin P, Burnstock G. Purinergic signalling: ATP release. *Neurochem Res*. 2001;26:959–969.
26. Sprague RS, Ellsworth ML, Stephenson AH, Lonigro AJ. ATP: the red blood cell link to NO and local control of the pulmonary circulation. *Am J Physiol*. 1996;271:H2717–H2722.
27. Ferguson DR, Kennedy I, Burton TJ. ATP is released from rabbit urinary bladder epithelial cells by hydrostatic pressure changes: a possible sensory mechanism? *J Physiol*. 1997;505:503–511.
28. Wang Y, Roman R, Lidofsky SD, Fitz JG. Autocrine signaling through ATP release represents a novel mechanism for cell volume regulation. *Proc Natl Acad Sci USA*. 1996;93:12020–12025.
29. Mitchell CH, Carre DA, McGlinn AM, et al. A release mechanism for stored ATP in ocular ciliary epithelial cells. *Proc Natl Acad Sci USA*. 1998;95:7174–7178.
30. Crosson CE, Gray T. Characterization of ocular hypertension induced by adenosine agonists. *Invest Ophthalmol Vis Sci*. 1996;37:1833–1839.
31. Lazarowski ER, Boucher RC, Harden TK. Mechanisms of release of nucleotides and integration of their action as P2X- and P2Y-receptor activating molecules. *Mol Pharmacol*. 2003;64:785–795.
32. Borst P, Elferink RO. Mammalian ABC transporters in health and disease. *Annu Rev Biochem*. 2002;71:537–592.
33. Rostovtseva T, Colombini M. VDAC channels mediate and gate the flow of ATP: implications for the regulation of mitochondrial function. *Biophys J*. 1997;72:1954–1962.
34. Stout CE, Costantin JL, Naus CC, Charles AC. Intercellular calcium signaling in astrocytes via ATP release through connexin hemichannels. *J Biol Chem*. 2002;10482–10488.
35. Braet K, Vandamme W, Martin PE, et al. Photoliberating inositol-1,4,5-trisphosphate triggers ATP release that is blocked by the connexin mimetic peptide gap 26. *Cell Calcium*. 2003;33:37–48.
36. Goodenough DA, Paul DL. Beyond the gap: functions of unpaired connexon channels. *Nat Rev Mol Cell Biol*. 2003;4:285–294.
37. Li F, Sugishita K, Su Z, et al. Activation of connexin-43 hemichannels can elevate $[Ca^{2+}]_i$ and $[Na^+]_i$ in rabbit ventricular myocytes during metabolic inhibition. *J Mol Cell Cardiol*. 2001;33:2145–2155.
38. Bonanno JA, Srinivas SP. Cyclic AMP activates anion channels in cultured bovine corneal endothelial cells. *Exp Eye Res*. 1997;64:953–962.
39. Bonanno JA, Giasson C. Intracellular pH regulation in fresh and cultured bovine corneal endothelium. II. Na^+:HCO_3^- cotransport and Cl^-/HCO_3^- exchange. *Invest Ophthalmol Vis Sci*. 1992;33:3068–3079.
40. MacCallum DK, Bahn CF, Lillie JH, et al. Evidence for corneal endothelial cell hypertrophy during postnatal growth of the cat cornea. *Invest Ophthalmol Vis Sci*. 1983;24:247–250.
41. Jans D, Srinivas SP, Waelkens E, et al. Hypotonic treatment evokes biphasic ATP release across the basolateral membrane of cultured renal epithelia (A6). *J Physiol*. 2002;545:543–555.
42. Leybaert L, Braet K, Vandamme W, et al. Connexin channels, connexin mimetic peptides and ATP release. *Cell Commun Adhes*. 2003;10:251–257.
43. Mohay J, McLaughlin BJ. Corneal endothelial wound repair in normal and mitotically inhibited cultures. *Graefes Arch Clin Exp Ophthalmol*. 1995;233:727–736.
44. Hofer A, Dermietzel R. Visualization and functional blocking of gap junction hemichannels (connexons) with antibodies against external loop domains in astrocytes. *Glia*. 1998;24:141–154.
45. Valiunas V. Biophysical properties of connexin-45 gap junction hemichannels studied in vertebrate cells. *J Gen Physiol*. 2002;119:147–164.
46. Guyot A, Hanrahan JW. ATP release from human airway epithelial cells studied using a capillary cell culture system. *J Physiol*. 2002;545:199–206.
47. Oike M, Droogmans G, Ito Y. ATP release pathways in vascular endothelial cells (in Japanese). *Nippon Yakurigaku Zasshi*. 2004;123:403–411.
48. Taylor AL, Kudlow BA, Marrs KL, et al. Bioluminescence detection of ATP release mechanisms in epithelia. *Am J Physiol*. 1998;275:C1391–C1406.
49. Wilson PD, Hovater JS, Casey CC, et al. ATP release mechanisms in primary cultures of epithelia derived from the cysts of polycystic kidneys. *J Am Soc Nephrol*. 1999;10:218–229.
50. Anderson CM, Bergher JP, Swanson RA. ATP-induced ATP release from astrocytes. *J Neurochem*. 2004;88:246–256.
51. Ito Y, Son M, Sato S, et al. ATP release triggered by activation of the Ca^{2+}-activated K^+ channel in human airway Calu-3 cells. *Am J Respir Cell Mol Biol*. 2004;30:388–395.
52. Coco S, Calegari F, Pravettoni E, et al. Storage and release of ATP from astrocytes in culture. *J Biol Chem*. 2003;278:1354–1362.
53. Takemura H, Takamura Y, Isono K, et al. Hypotonicity-induced ATP release is potentiated by intracellular Ca^{2+} and cyclic AMP in cultured human bronchial cells. *Jpn J Physiol*. 2003;53:319–326.
54. Olearczyk JJ, Stephenson AH, Lonigro AJ, Sprague RS. Heterotrimeric G protein G_i is involved in a signal transduction pathway for ATP release from erythrocytes. *Am J Physiol.* 2004;286:H940–H945.
55. Boudreault F, Grygorczyk R. Cell swelling-induced ATP release and gadolinium-sensitive channels. *Am J Physiol*. 2002;282:C219–C226.
56. Stout C, Charles A. Modulation of intercellular calcium signaling in astrocytes by extracellular calcium and magnesium. *Glia*. 2003;43:265–273.
57. Suh BC, Kim JS, Namgung U, et al. P2X7 nucleotide receptor mediation of membrane pore formation and superoxide generation in human promyelocytes and neutrophils. *J Immunol*. 2001;166:6754–6763.
58. Fortes FS, Pecora IL, Persechini PM, et al. Modulation of intercellular communication in macrophages: possible interactions between GAP junctions and P2 receptors. *J Cell Sci.* 2004;117:4717–4726.
59. Steinberg TH, Newman AS, Swanson JA, Silverstein SC. ATP_4^- permeabilizes the plasma membrane of mouse macrophages to fluorescent dyes. *J Biol Chem*. 1987;262:8884–8888.
60. Nuttle LC, Dubyak GR. Differential activation of cation channels and non-selective pores by macrophage P2z purinergic receptors expressed in Xenopus oocytes. *J Biol Chem*. 1994;269:13988–13996.
61. Duan S, Anderson CM, Keung EC, et al. P2X7 receptor-mediated release of excitatory amino acids from astrocytes. *J Neurosci*. 2003;23:1320–1328.

62. Srinivas SP, Ong A, Goon L, Bonanno JA. Lysosomal Ca^{2+} stores in bovine corneal endothelium. *Invest Opbthalmol Vis Sci*. 2002;43: 2341–2350.
63. Srinivas SP, Bonanno JA, Hughes BA. Assessment of swelling-activated Cl− channels using the halide-sensitive fluorescent indicator 6-methoxy-N-(3-sulfopropyl)quinolinium. *Biophys J*. 1998; 75:115–123.
64. Braet K, Aspeslagh S, Vandamme W, et al. Pharmacological sensitivity of ATP release triggered by photoliberation of inositol-1,4,5-trisphosphate and zero extracellular calcium in brain endothelial cells. *J Cell Physiol*. 2003;197:205–213.
65. Williams K, Watsky M. Gap junctional communication in the human corneal endothelium and epithelium. *Curr Eye Res*. 2002;25: 29–36.
66. Lazarowski ER, Homolya L, Boucher RC, Harden TK. Direct demonstration of mechanically induced release of cellular UTP and its implication for uridine nucleotide receptor activation. *J Biol Chem*. 1997;272:24348–24354.
67. Joseph SM, Buchakjian MR, Dubyak GR. Colocalization of ATP release sites and ecto-ATPase activity at the extracellular surface of human astrocytes. *J Biol Chem*. 2003;278:23331–23342.
68. Lazarowski ER, Boucher RC, Harden TK. Constitutive release of ATP and evidence for major contribution of ecto-nucleotide pyrophosphatase and nucleoside diphosphokinase to extracellular nucleotide concentrations. *J Biol Chem*. 2000;275:31061–31068.
69. Beigi R, Kobatake E, Aizawa M, Dubyak GR. Detection of local ATP release from activated platelets using cell surface-attached firefly luciferase. *Am J Physiol*. 1999;276:C267–C278.
70. Bodin P, Burnstock G. Evidence that release of adenosine triphosphate from endothelial cells during increased shear stress is vesicular. *J Cardiovasc Pharmacol*. 2001;38:900–908.
71. Gatof D, Kilic G, Fitz JG. Vesicular exocytosis contributes to volume-sensitive ATP release in biliary cells. *Am J Physiol*. 2004; 286:G538–G546.
72. Abdipranoto A, Liu GJ, Werry EL, Bennett MR. Mechanisms of secretion of ATP from cortical astrocytes triggered by uridine triphosphate. *Neuroreport*. 2003;14:2177–2181.
73. Abraham EH, Prat AG, Gerweck L, et al. The multidrug resistance (mdr1) gene product functions as an ATP channel. *Proc Natl Acad Sci U S A*. 1993;90:312–316.
74. Reisin IL, Prat AG, Abraham EH, et al. The cystic fibrosis transmembrane conductance regulator is a dual ATP and chloride channel. *J Biol Chem*. 1994;269:20584–20591.
75. Sabirov RZ, Dutta AK, Okada Y. Volume-dependent ATP-conductive large-conductance anion channel as a pathway for swelling-induced ATP release. *J Gen Physiol*. 2001;118:251–266.
76. Hisadome K, Koyama T, Kimura C, et al. Volume-regulated anion channels serve as an auto/paracrine nucleotide release pathway in aortic endothelial cells. *J Gen Physiol*. 2002;119:511–520.
77. Bruzzone R, Hormuzdi SG, Barbe MT, et al. Pannexins, a family of gap junction proteins expressed in brain. *Proc Natl Acad Sci USA*. 2003;100:13644–13649.
78. Bao L, Locovei S, Dahl G. Pannexin membrane channels are mechanosensitive conduits for ATP. *FEBS Letts*. 2004;572:65–68.
79. John SA, Kondo R, Wang SY, et al. Connexin-43 hemichannels opened by metabolic inhibition. *J Biol Chem*. 1999;274:236–240.